Supporting Information

Three New Metastable Polymorphs of 1-(9-Anthryl)-2-(1-naphthyl)ethylene and the Polymorph-Dependent Phase Transition and Fluorescence Change Property

Ye-Xin Li,* Zhen-Feng Yu, Cun-Zhao Zhu, Xiao-Feng Yang, Yong Nie, Yu Cui and Guo-Xin Sun*

General information

^{1}H NMR spectra were conducted on a Bruker Avance 400 spectrometer. Differential scanning calorimetry (DSC) analyses were measured on Netzsch DSC 200F3 or Netzsch DSC 214 Polyma instrument. Thermogravimetric (TG) analyses were measured on a Netzsch5 instrument, in a flowing nitrogen atmosphere and with a 15 ºC min^{-1} to 450 ºC. Single-crystal X-ray diffraction measurements were measured on a Bruker D8 Venture diffractometer with Ga K_α radiation (λ = 1.34139 Å). The absorption correction was applied using SADABS program.[1] The structure was solved by direct method and refined by a full-matrix least-squares technique on F^2 using SHELXL-97 programs.[2,3] CCDC-1818417 (**ANE-e**) contains the supplementary crystallographic data for this paper. Powder X-ray diffraction (PXRD) investigations were carried out on a D8 Focus diffractometer equipped with Cu K_α radiation (λ = 1.5406 Å) using a XRD silicon holder. Profile fitting analyses were performed using TOPAS software.

All calculations were performed with the program package Gaussian 09.[4] The ground-state (S_0) geometry was optimized in the gas phase using density functional theory (DFT) at the B3LYP/6-31G(d) level. Using the optimized ground-state geometry as initial structure, the first excited-state (S_1) geometry was optimized

using time-dependent density functional theory (TD-DFT) at the B3LYP/6-31G(d) level. No symmetry constraint was used during the geometry optimization. Frequency calculations were performed on all minima to check the absence of negative frequency.

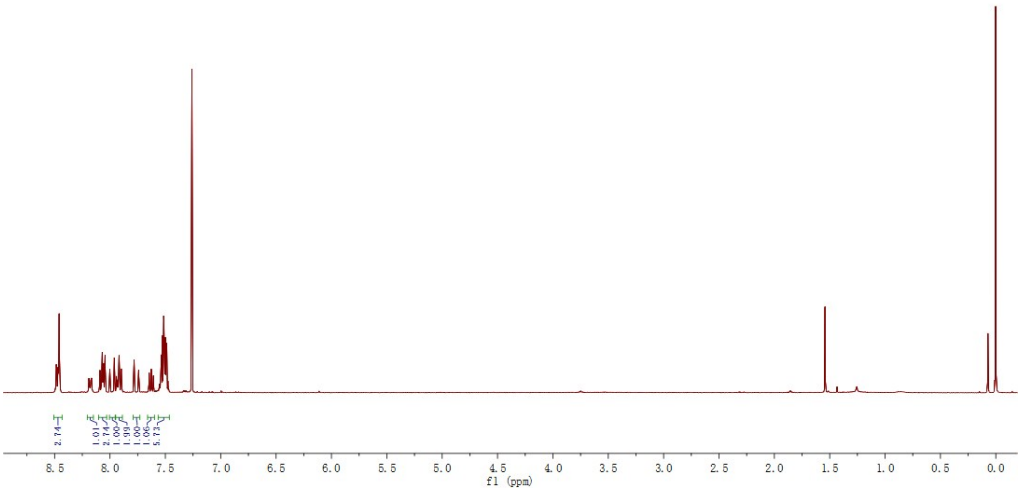

Figure S1. ^{1}H NMR spectrum of **ANE-d** in $CDCl_3$ solution.

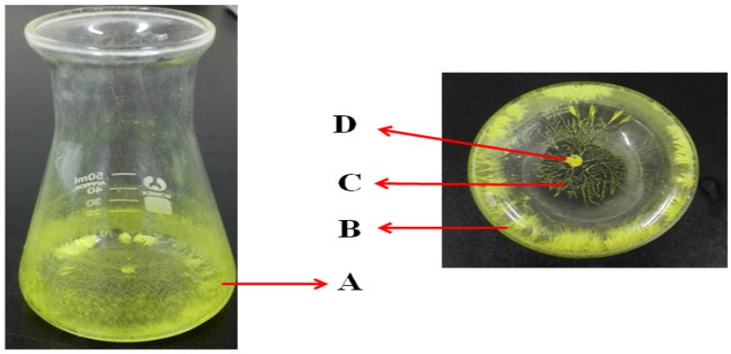

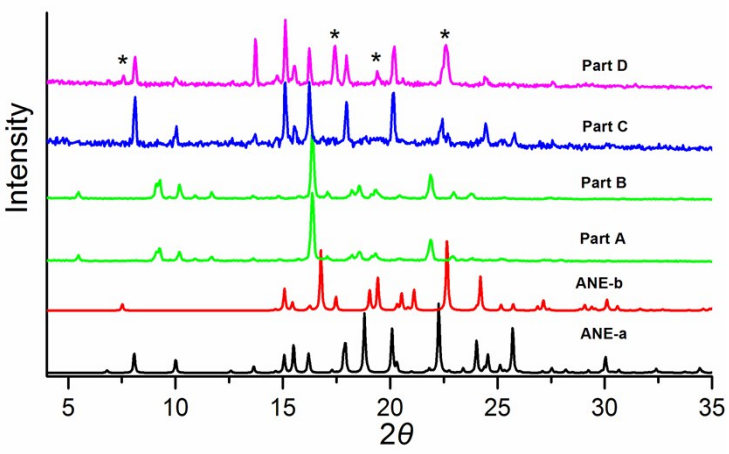

Figure S2. Photographs of **ANE** crystals grown from ethyl ether solution in a conical flask and the PXRD patterns of crystals in different part of the container. For comparison, the calculated diffraction spectra of **ANE-a** and **ANE-b** are also present.

As can be seen from the PXRD result, crystals from parts A and B are polymorph **ANE-e**. Crystals from part C are polymorph **ANE-a**. Crystals from part D are a mixture of polymorphs **ANE-a** and **ANE-b**. The diffraction peaks labelled with * correspond to **ANE-b**.

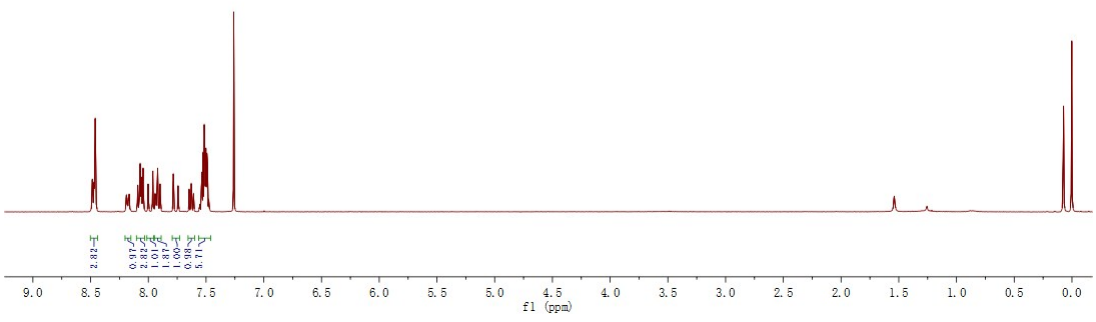

Figure S3. The ^{1}H NMR spectrum of **ANE-e** in $CDCl_3$ solution.

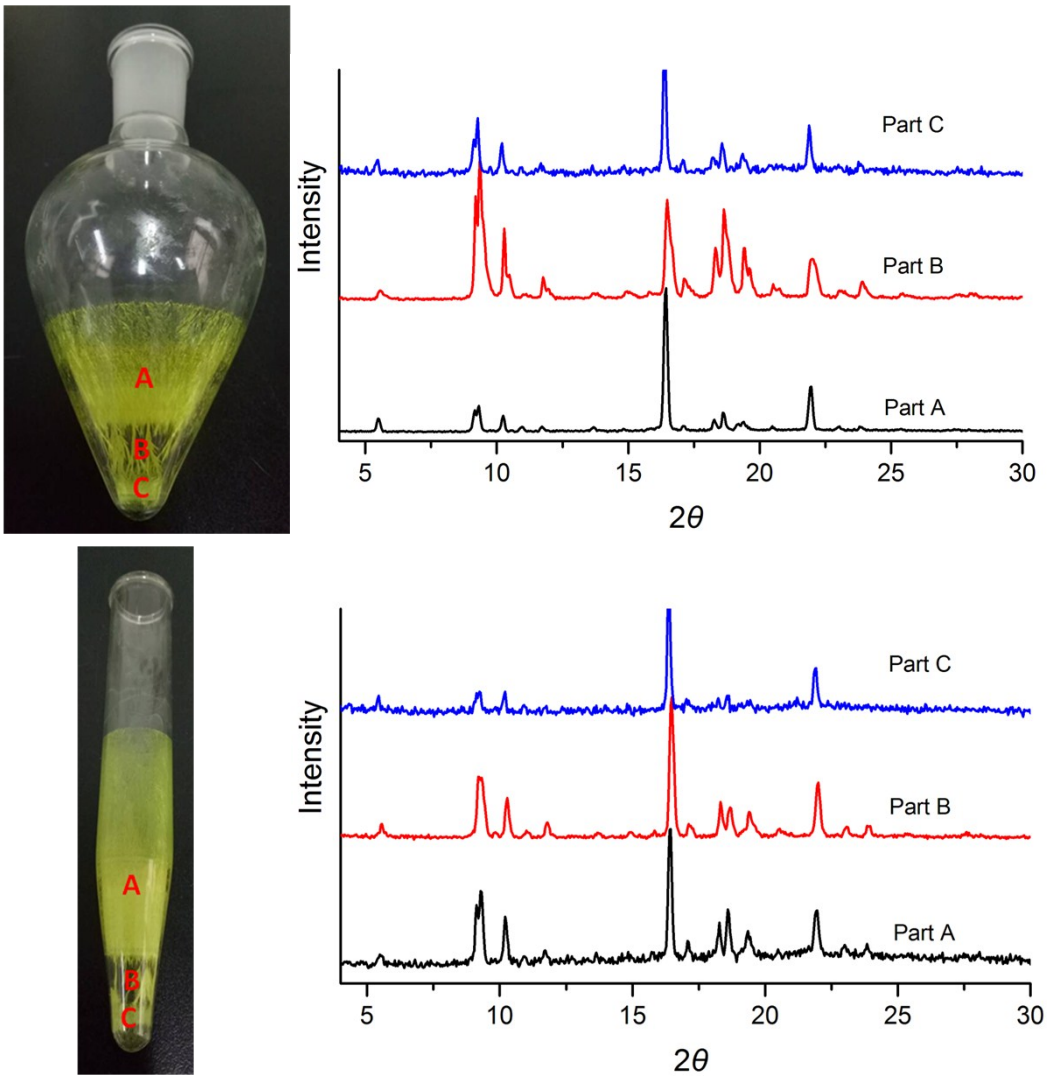

Figure S4. Photographs of **ANE** crystals grown from ethyl ether solution in pear-shaped flask and centrifuge tube. The PXRD patterns of crystals in different part of the container were measured. All the XRD patterns are in good agreement with **ANE-e**.

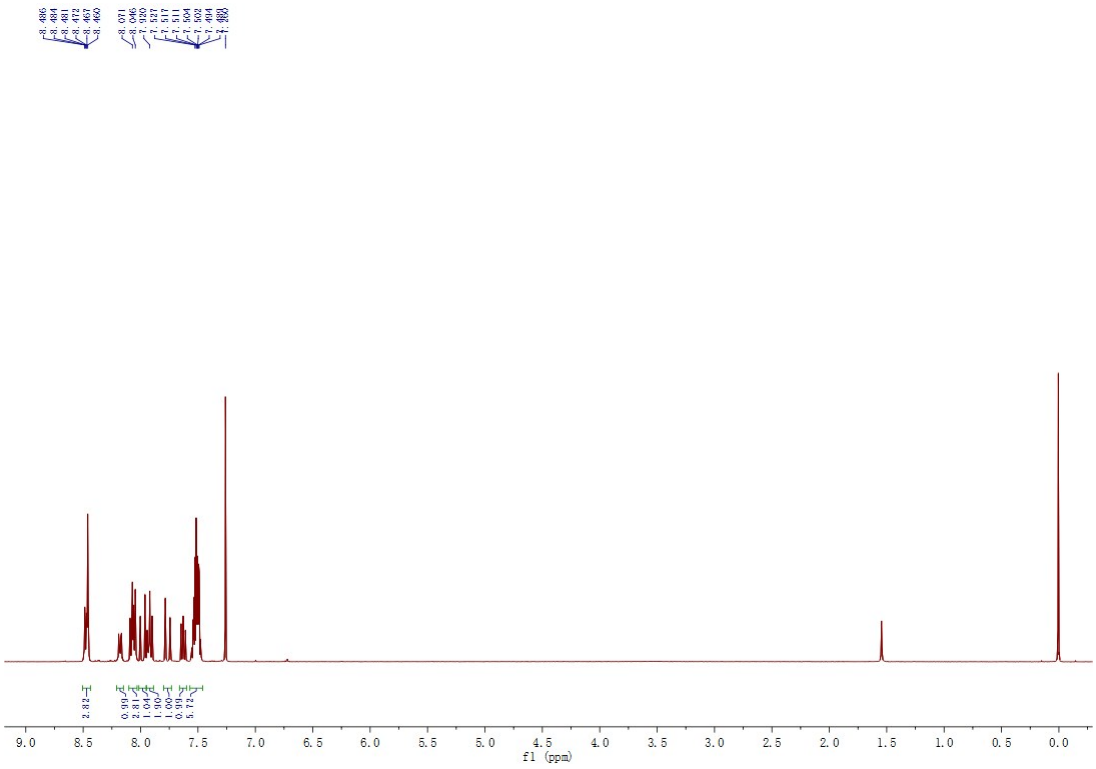

Figure S5. The ^{1}H NMR spectrum of **ANE-f** in $CDCl_3$ solution.

Table S1. The fluorescence lifetimes of **ANE-d**, **ANE-e**, and **ANE-f**.

Compound	Lifetime(ns)
ANE-d	0.91(61%), 3.26(39%)
ANE-e	1.19(60%), 3.86(40%)
ANE-f	1.36(41%), 3.07(59%)

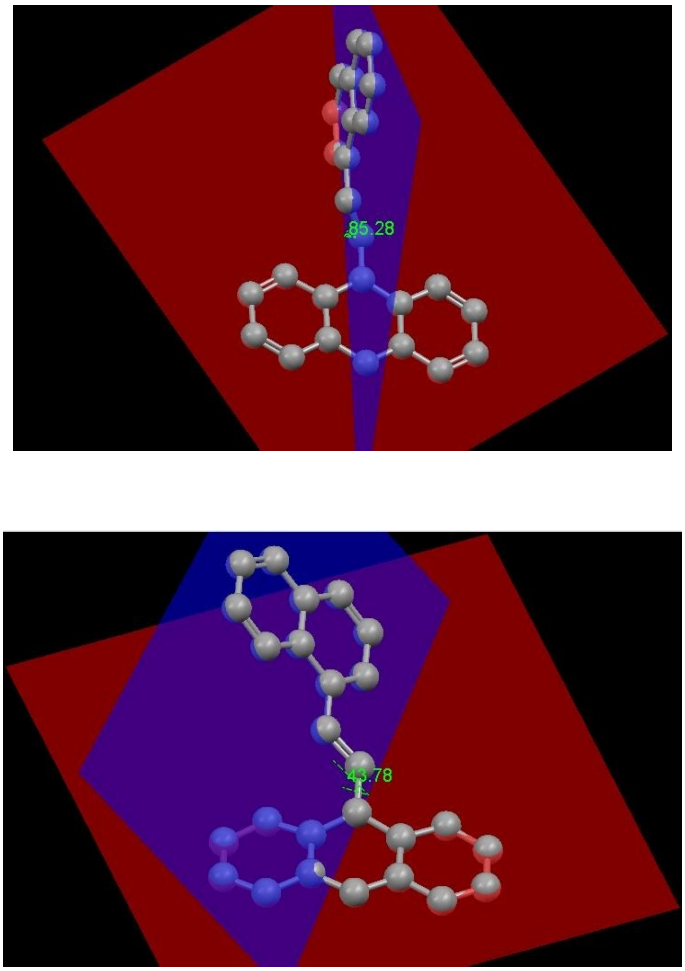

Figure S6. The calculated molecular structures of **ANE** in ground (upper) and first excited (lower) states.

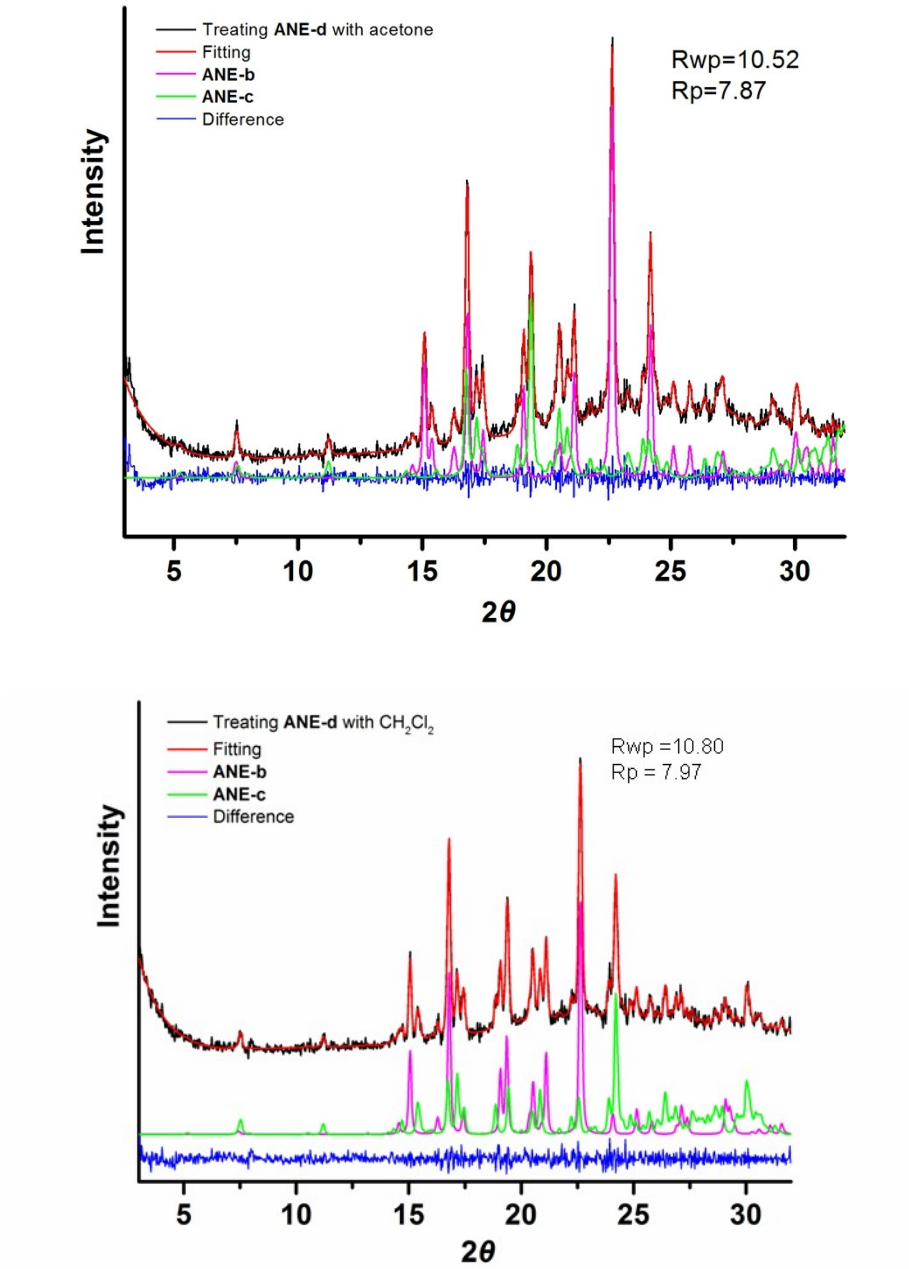

Figure S7. Profile fitting of the PXRD pattern of **ANE-d** sample after organic solvent vapour fuming**.**

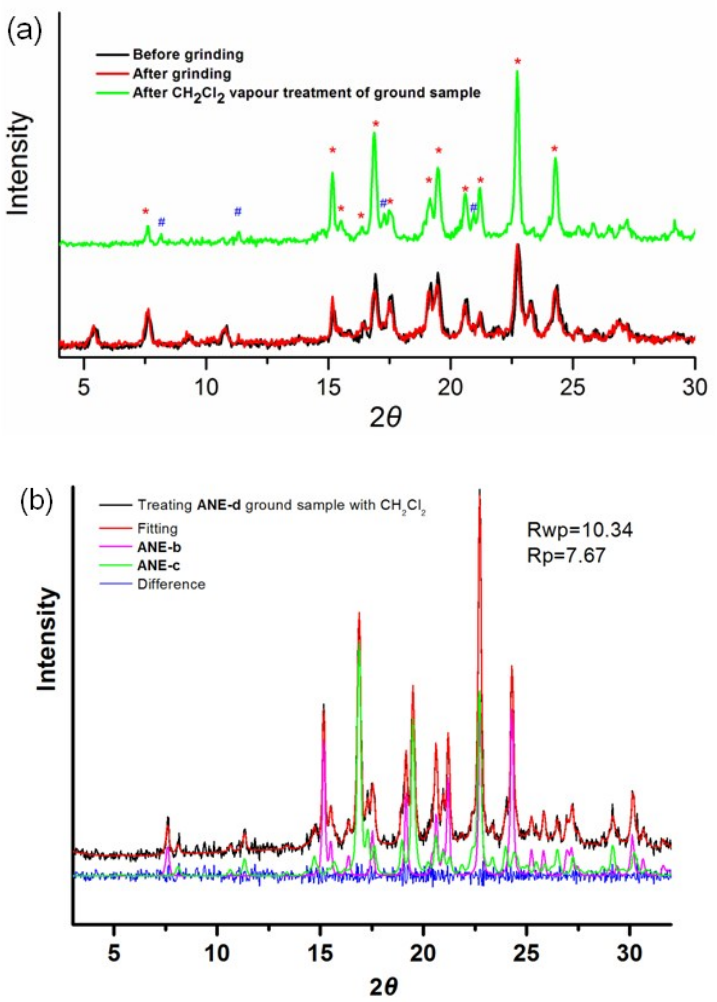

Figure S8. (a) XRD patterns of **ANE-d** sample with different treatment. The diffraction peaks labelled with * belong to **ANE-b**. The diffraction peaks labelled with # correspond to **ANE-c**. (b) Profile fitting of the PXRD pattern of **ANE-d** ground sample after CH_2Cl_2 fuming**.**

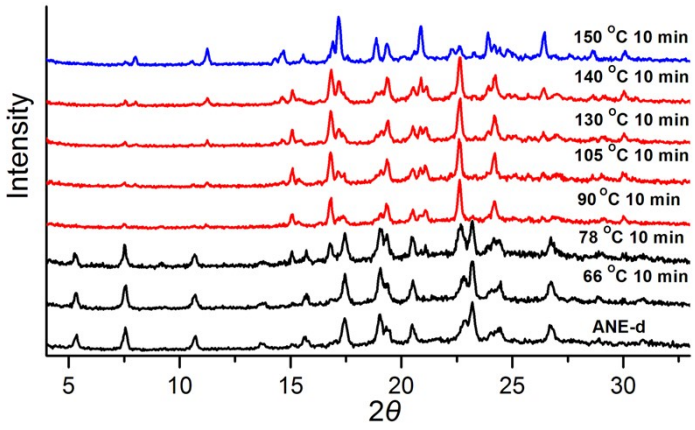

Figure S9. The change of XRD patterns with temperature upon heating **ANE-d** powder.

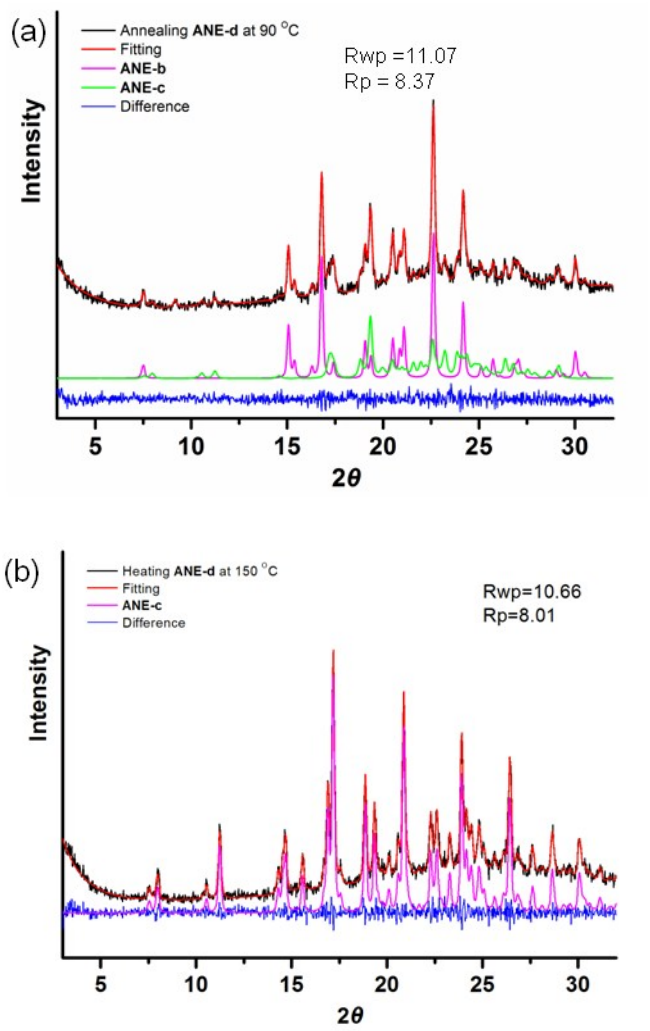

Figure S10. Profile fitting of the PXRD pattern of **ANE-d** sample after annealing at 90 °C (a) and 150 °C (b), respectively**.**

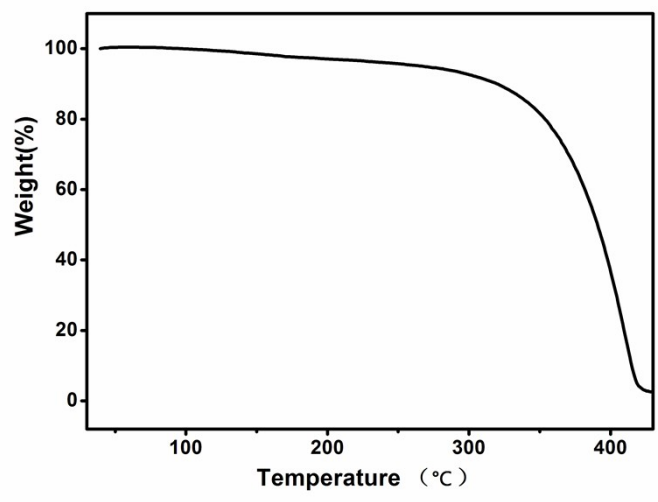

Figure S11. TG curves of **ANE-d**. The heating rate is 15 ℃/min.

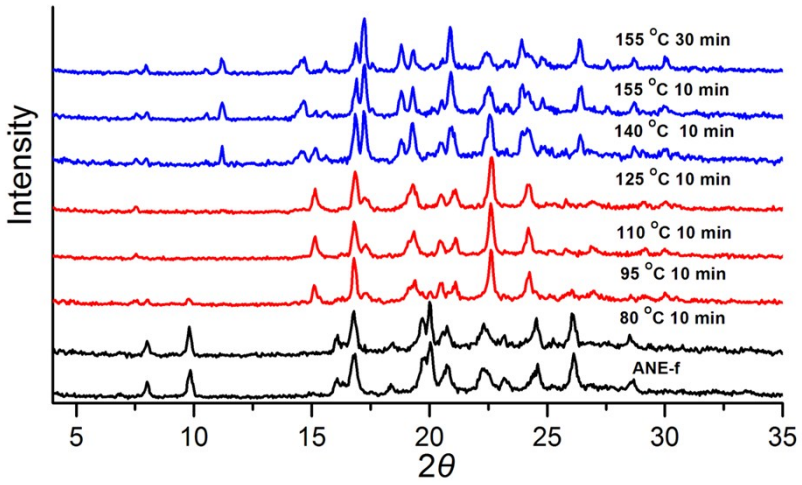

Figure S12. The change of PXRD pattern with temperature upon heating **ANE-f** sample.

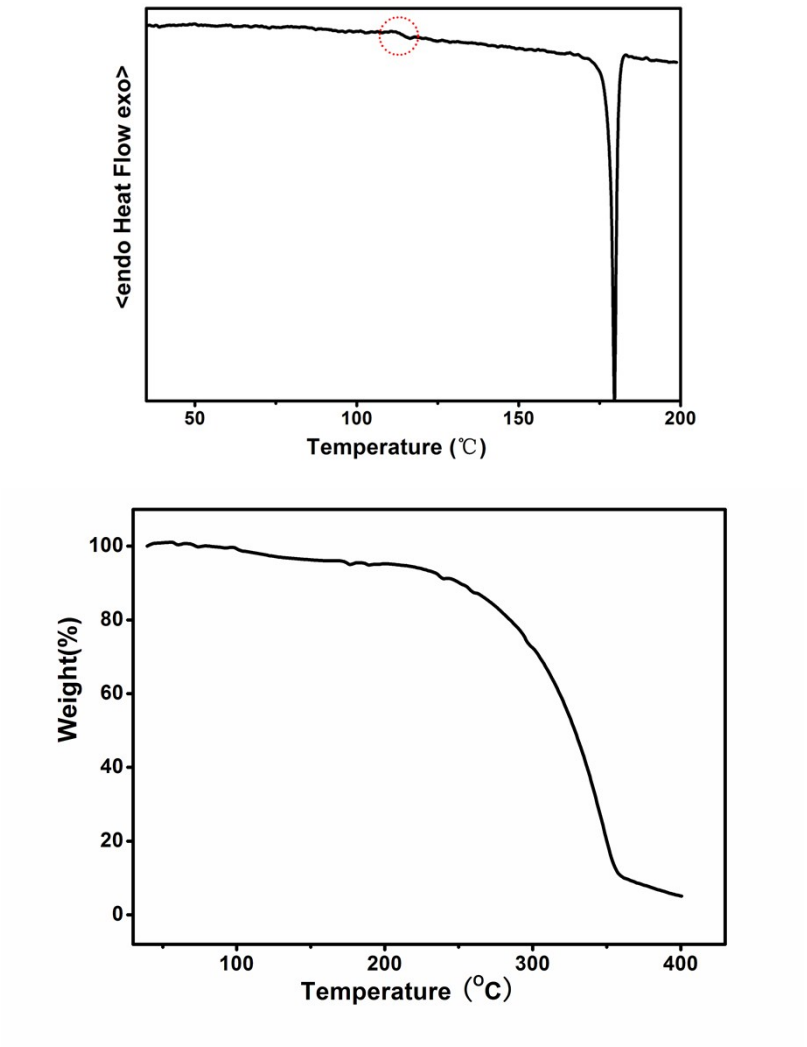

Figure S13. DSC and TG curves of **ANE-f**. The heating rate is 3 ºC/min for DSC and 15 ºC/min for TG measurement.

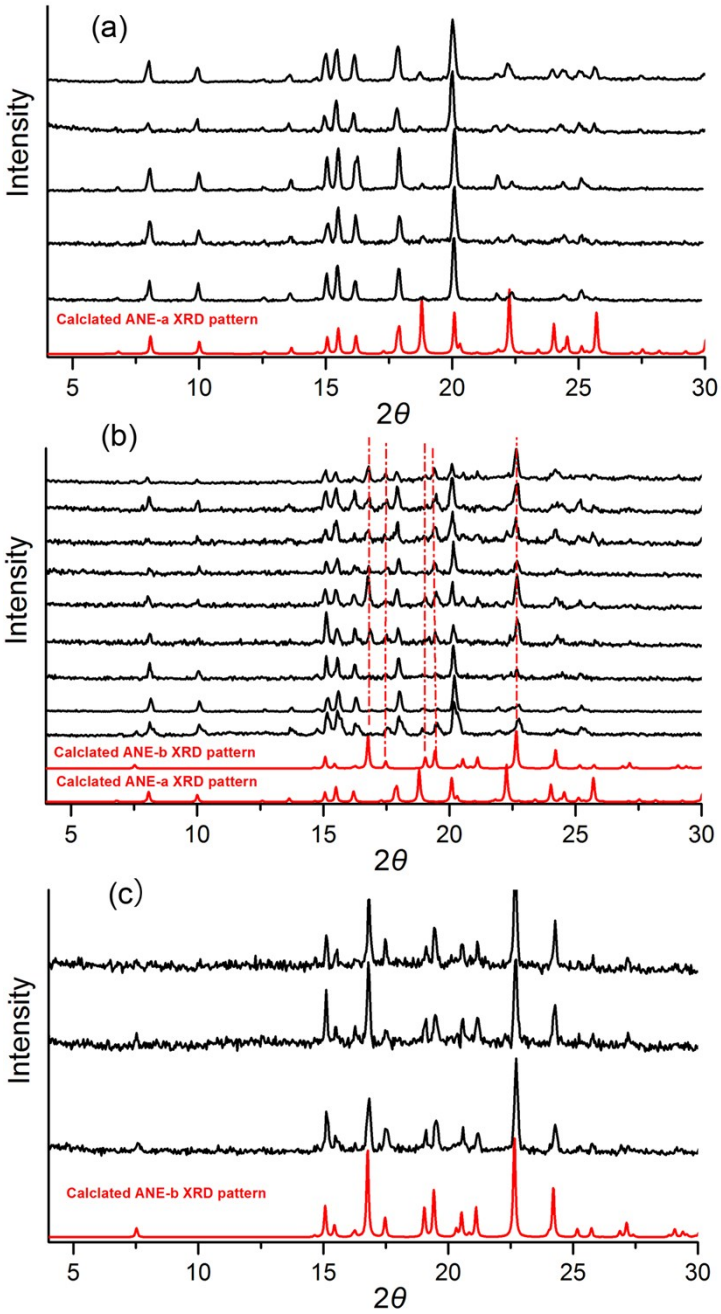

Figure S14. PXRD patterns of the seventeen batches of **ANE-e** crystal samples after treating with CH_2Cl_2 vapour: (a) five batches of samples transform to **ANE-a**, (b) nine batches of samples convert to a mixture of **ANE-a** and **ANE-b**, and (c) three batches of samples transform to **ANE-b**. For comparison, the calculated diffraction spectra of **ANE-a** and **ANE-b** are also present.

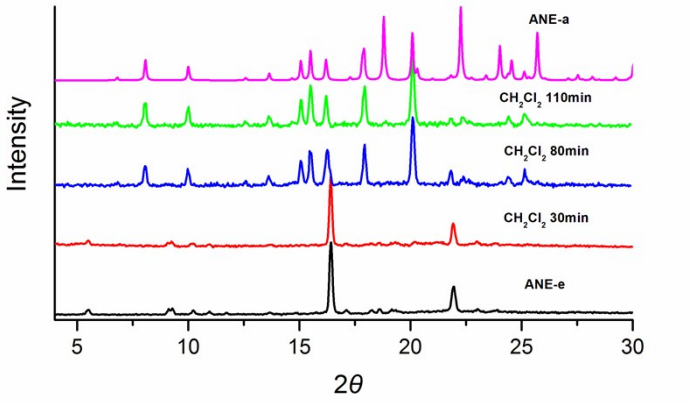

Figure S15. PXRD pattern change with time for as-grown **ANE-e** crystals during CH_2Cl_2 vapour-mediated polymorphic transformation. For comparison, the calculated diffraction spectrum of **ANE-a** is present.

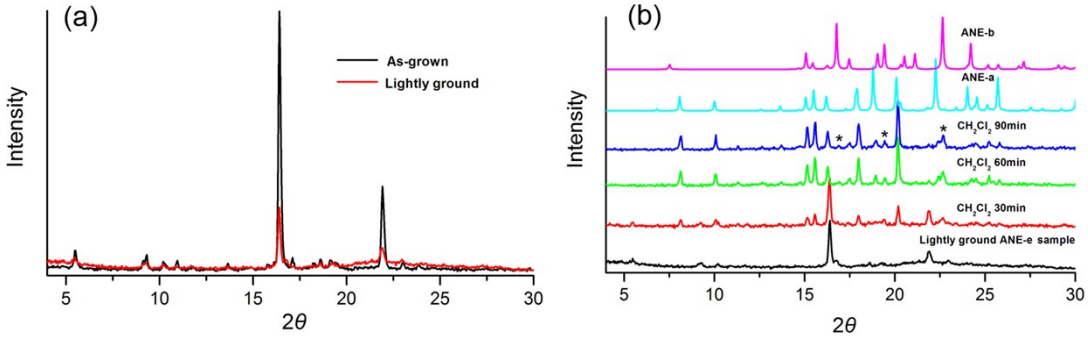

Figure S16. (a) PXRD patterns of **ANE-e** sample before and after lightly grinding. The as-grown crystal sample was ground directly on the XRD silicon holder. (b) PXRD pattern change with time for the lightly ground **ANE-e** sample during CH_2Cl_2 vapour-mediated polymorphic transformation. For comparison, the calculated diffraction spectra of **ANE-a** and **ANE-b** are present. The characteristic diffraction peaks of **ANE-b** are labelled with *.

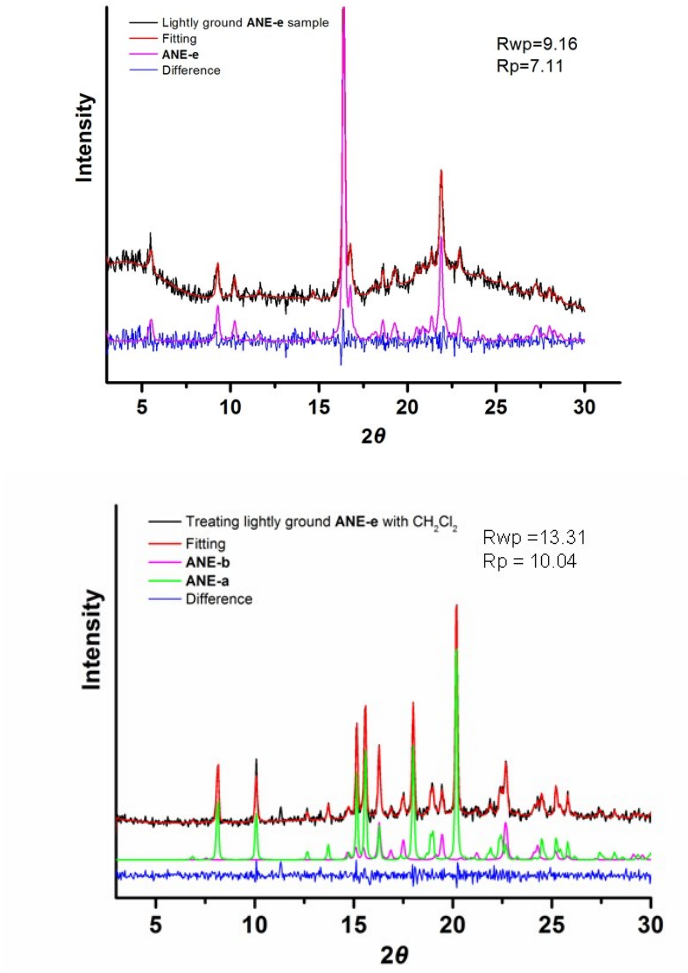

Figure S17. Profile fitting of the PXRD pattern of lightly ground **ANE-e** sample before and after CH_2Cl_2 fuming**.**

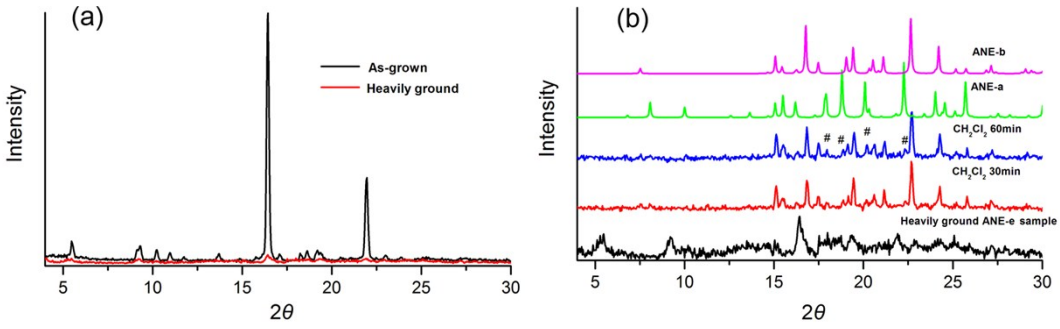

Figure S18. (a) The comparison of PXRD patterns of **ANE-e** sample before and after heavily grinding. The as-grown crystal sample was ground directly on the XRD silicon holder. (b) PXRD pattern change with time for heavily ground **ANE-e** sample during CH_2Cl_2 vapour-mediated polymorphic transformation. For comparison, the calculated diffraction spectra of **ANE-a** and **ANE-b** are present. The characteristic diffraction peaks of **ANE-a** are labelled with #.

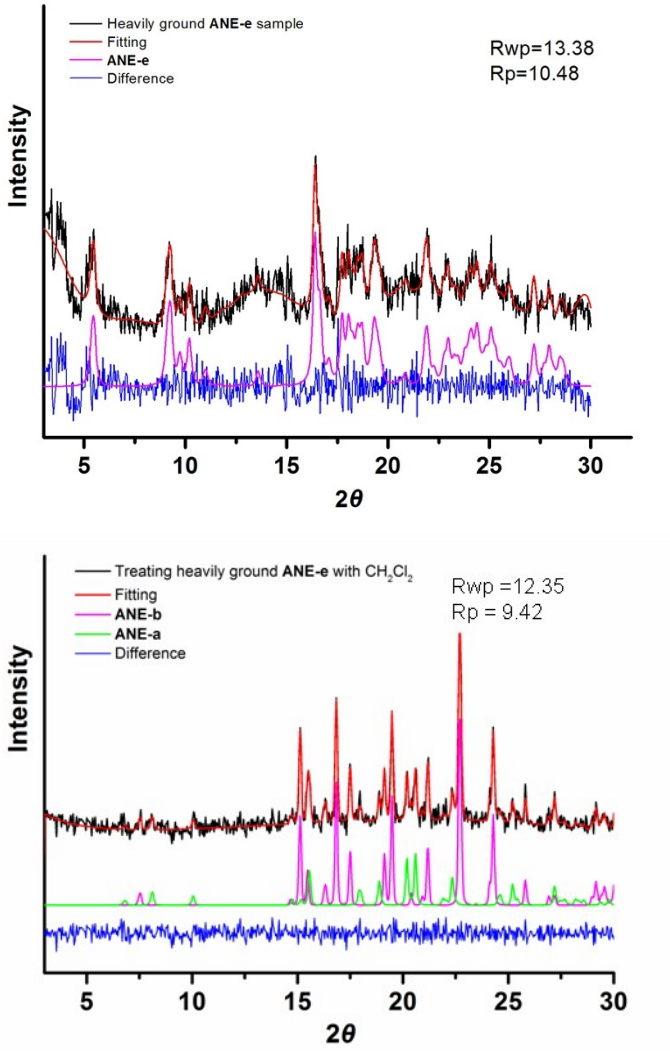

Figure S19. Profile fitting of the PXRD pattern of heavily ground **ANE-e** sample before and after CH_2Cl_2 fuming**.**

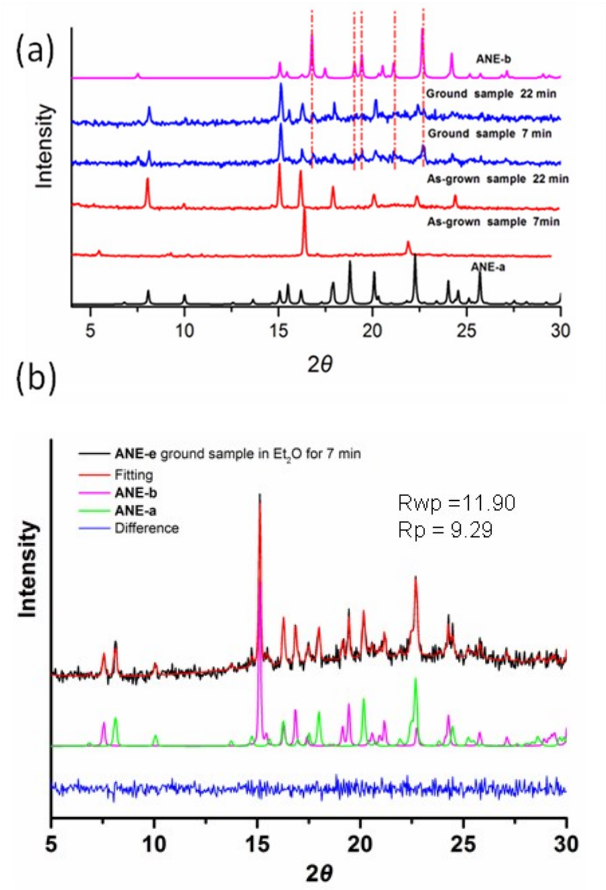

Figure S20. (a) PXRD pattern changes for **ANE-e** as-grown and ground samples extracted from saturated ethyl ether solution at different period of time. For comparison, the calculated diffraction spectra of **ANE-a** and **ANE-b** are also present. (b) Profile fitting of the PXRD pattern of **ANE-e** ground sample after dipping in ethyl ether solution for 7 minutes.

This solvent-mediated polymorphic transformation of polymorph **ANE-e** was carried out in ethyl ether saturated solution. A small amount of as-grown and ground samples (about 5 mg) were respectively dipped in saturated ethyl ether solution, which was sealed in a plastic centrifuge tube (volume 2 mL). After a certain period of time, the solution was removed and the solid was immediately detected by XRD. The ground sample transforms to a mixture of **ANE-a** and **ANE-b** within 7 minutes, while no phase transition was detected for the as-grown sample. The latter finally transforms to polymorph **ANE-a** after dipping for another 15 minutes.

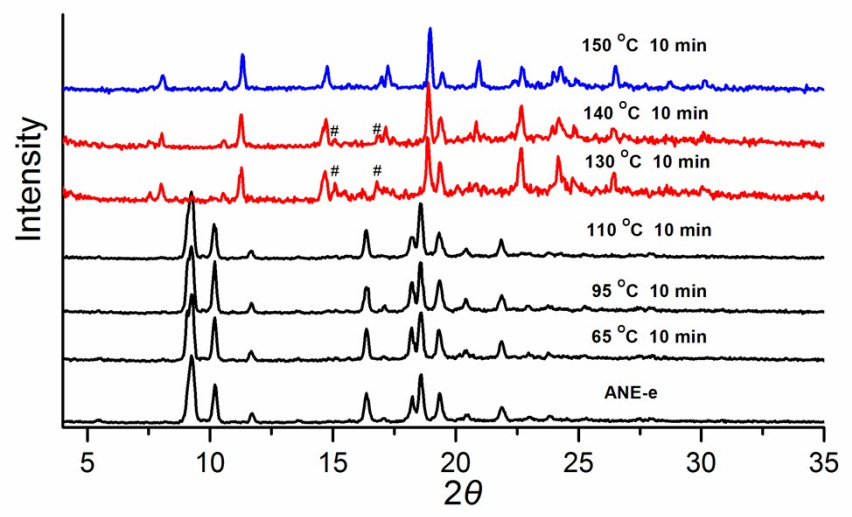

Figure S21. The change of XRD patterns with temperature upon heating **ANE-e** powder. The weak diffraction peaks at 2θ = 15.1 and 16.8° (labeled with #) correspond to polymorph **ANE-b**.

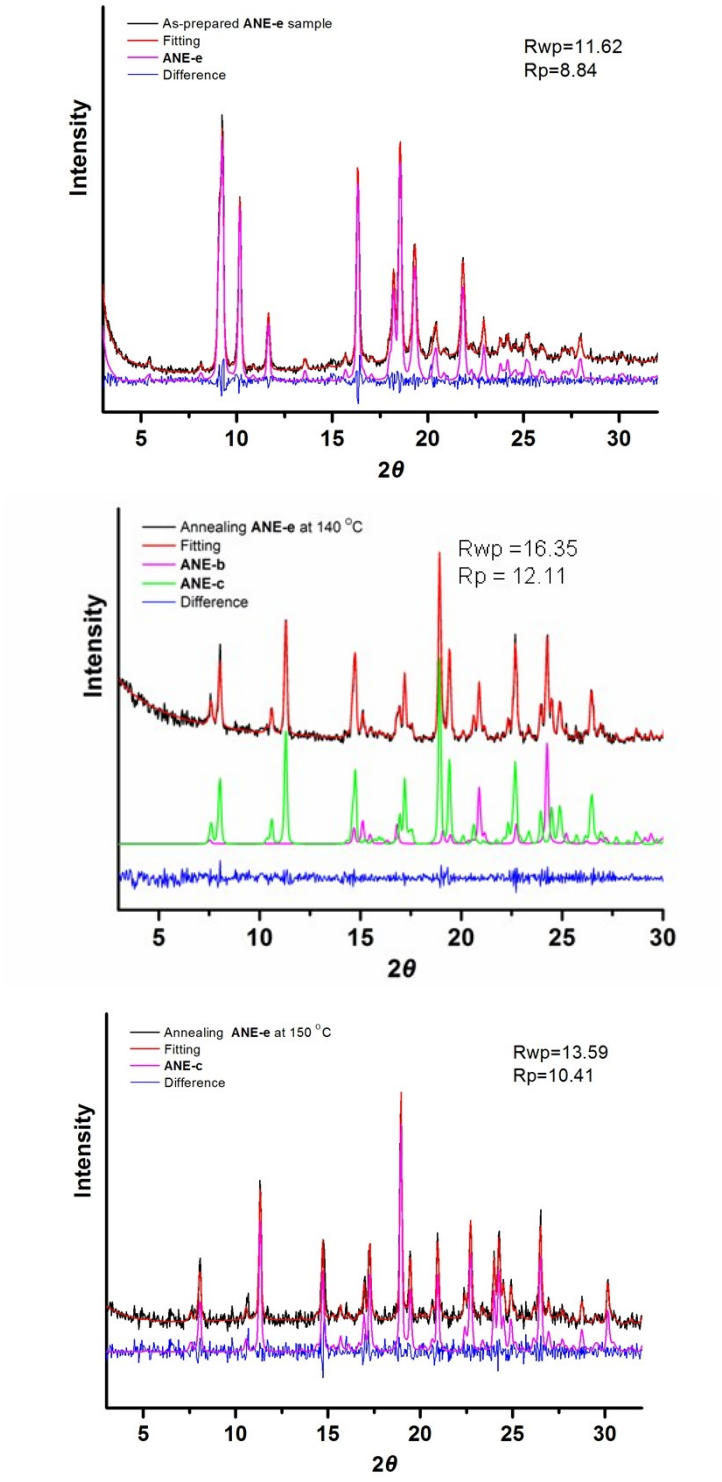

Figure S22. Profile fitting of the PXRD pattern of as-prepared **ANE-e** sample and **ANE-e** samples after annealing at 140 °C and 150 °C, respectively**.**

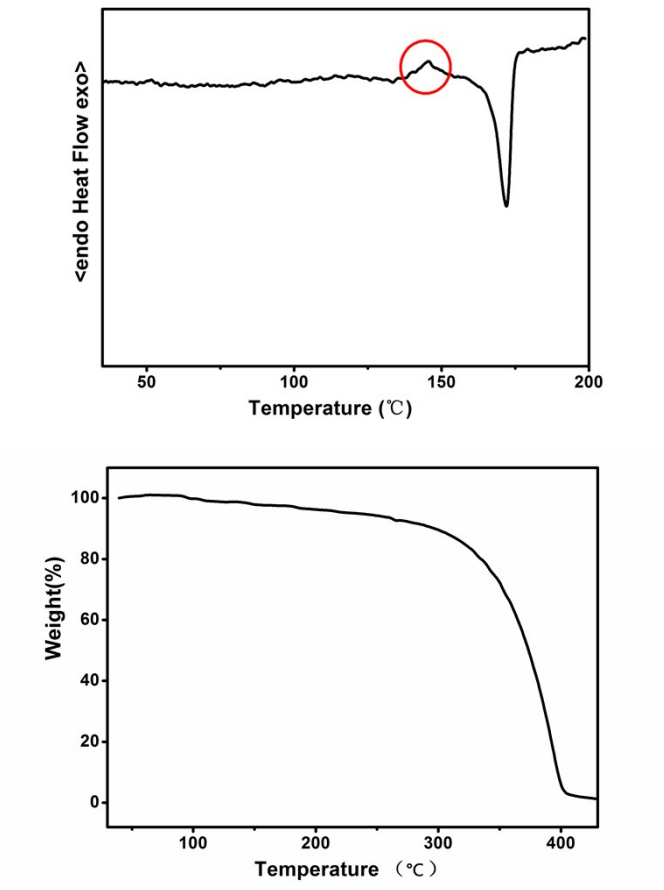

Figure S23. DSC and TG curves of **ANE-e**. The heating rate is 3 ºC/min for DSC and 15 ºC/min for TG measurement.

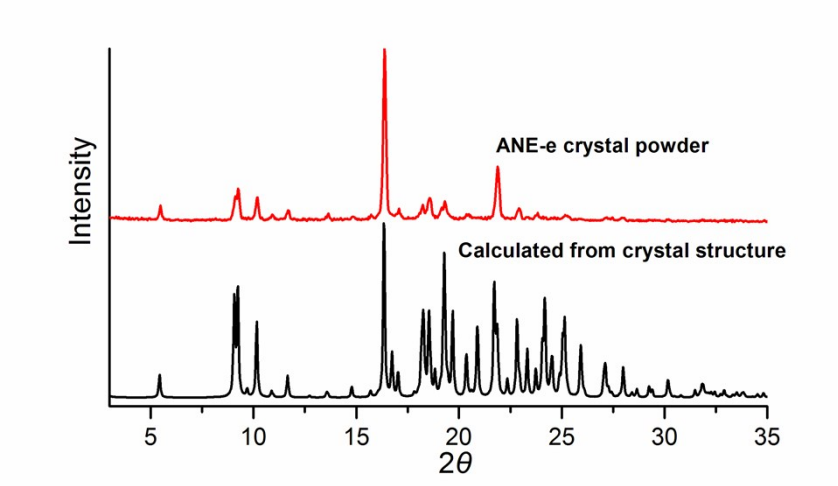

Figure S24. The PXRD patterns of **ANE-e** crystals and its simulated diffractogram based on single-crystal structure.

Table S2. The cell parameters of **ANE-a**, **ANE-e**, and **ANE-b**.

Compound	**ANE-a**	**ANE-e**	**ANE-b**
CCDC number	885362	1818417	885363
Chemical formula	C26H18	C26H18	C13H9
Formula Mass	330.40	330.40	165.20
Crystal system	Orthorhombic	Monoclinic	Monoclinic
a/Å	5.5771(3)	9.7845(147)	12.5169(17)
b/Å	12.0652(6)	5.5978(8)	6.1861(7)
c/Å	25.9356(12)	32.633(5)	12.2167(18)
α/°	90	90.00	90
β/°	90	95.028(10)	110.239(15)
γ/°	90	90.00	90
Unit cell volume/Å^3	1745.18(15)	1780.5(4)	887.5(2)
Space group	$P2_12_12_1$	$P2_1$	$P2_1/c$
Temperature/K	293(2)	296(2)	293(2)
No. of formula units per unit cell, Z	4	4	4
No. of reflections measured	5686	43681	4208
No. of independent reflections	2083	6700	1815
R_{int}	0.0393	0.2351	0.0212
Final R_1 values ($I > 2\sigma(I)$)	0.0474	0.0799	0.0617
Final $wR(F^2)$ values ($I > 2\sigma(I)$)	0.0858	0.1551	0.1420
Final R_1 values (all data)	0.0870	0.2605	0.1165
Final $wR(F^2)$ values (all data)	0.0995	0.2312	0.1743
Goodness of fit on F^2	0.980	0.960	1.037
Flack parameter	-	0(4)	-

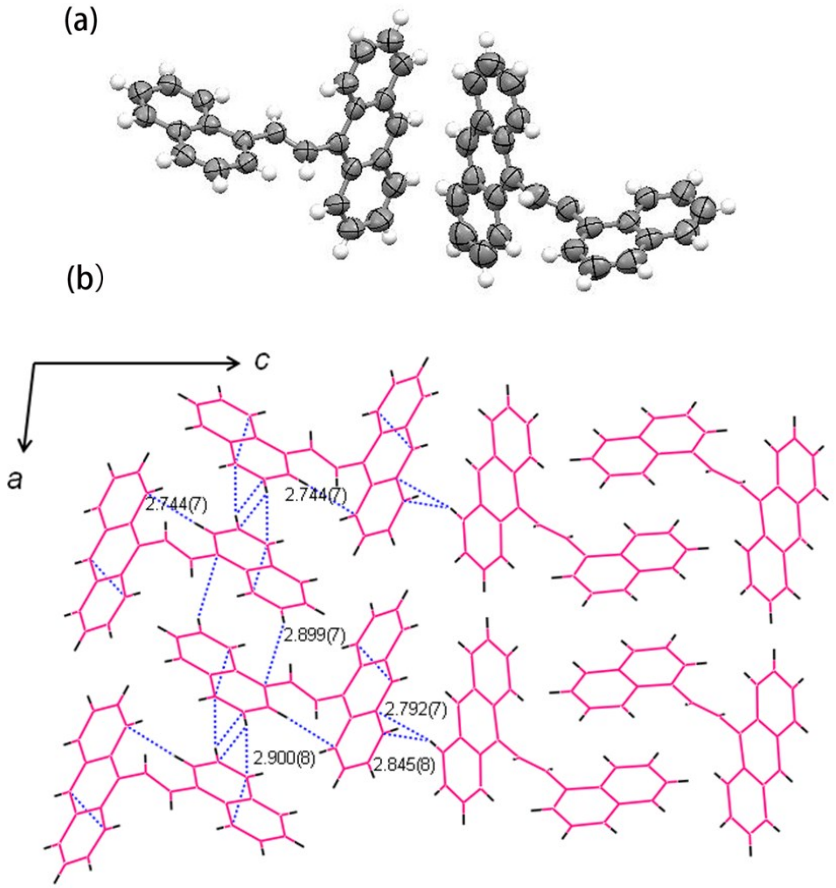

Figure S25. (a) The structures of two symmetry-independent molecules per asymmetric unit with thermal ellipsoids at the 50 % probability level. (b) **ANE-e** molecules packing in the *ac* plane. The C–H···π interactions are labelled by blue dotted line. The distance unit is Å.

References:

1. G. M. Sheldrick, *SADABS: An Empirical Absorption Correction Program for Area Detector Data*; University of Göttingen: Göttingen, Germany, **1996**.

2. G. M. Sheldrick, *Acta Crystallogr*., *Sect. A: Found. Crystallogr.* **2008**, *64*, 112-122.

3. O. V. Dolomanov, L. J. Bourhis, R. J. Gildea, J. A. K. Howard, H. Puschmann, *J. Appl. Crystallogr*. **2009**, *42*, 339-341.

4. M. J. Frisch, G. W. Trucks, H. B. Schlegel, G. E. Scuseria, M. A. Robb, J. R.

Cheeseman, G. Cheeseman, V. Barone, B. Mennucci, G. A. Petersson, H. Nakatsuji, M. Caricato, X. Li, H. P. Hratchian, A. F. Izmaylov, J. Bloino, G. Zheng, J. L. Sonnenberg, M. Hada, M. Ehara, K. Toyota, R. Fukuda, J. Hasegawa, M. Ishida, T. Nakajima, Y. Honda, O. Kitao, H. Nakai, T. Vreven, J. A. Montgomery, J. J. E. Peralta, F. Ogliaro, M. Bearpark, J. J. Heyd, E. Brothers, K. N. Kudin, V. N. Staroverov, R. Kobayashi, J. Normand, K. Raghavachari, A. Rendell, J. C. Burant, S. S. Iyengar, J. Tomasi, M. Cossi, N. Rega, J. M. Millam, M. Klene, J. E. Knox, J. B. Cross, V. Bakken, C. Adamo, J. Jaramillo, R. Gomperts, R. E. Stratmann, O. Yazyev, A. J. Austin, R. Cammi, C. Pomelli, J.W. Ochterski, R. L. Martin, K. Morokuma, V. G. Zakrzewski, G. A. Voth, P. Salvador, J. Dannenberg, S. Dapprich, A. D. Daniels, O. Farkas, J. B. Foresman, J. V. Ortiz, J. Cioslowski, D. J. Fox, *Gaussian 09*, Revision A.02. Wallingford CT: Gaussian, Inc; 2009.